

SANDIA REPORT

SAND2005-2638

Unlimited Release

Printed September 2006

Final Report on Development of Pulse Arrested Spark Discharge (PASD) for Aging Aircraft Wiring Application

R. Kevin Howard, Steven F. Glover, Gary E. Pena, Matthew B. Higgins,
Larry X Schneider and Thomas R. Lockner

Prepared by
Sandia National Laboratories
Albuquerque, New Mexico 87185 and Livermore, California 94550

Sandia is a multiprogram laboratory operated by Sandia Corporation,
a Lockheed Martin Company, for the United States Department of Energy's
National Nuclear Security Administration under Contract DE-AC04-94AL85000.

Approved for public release; further dissemination unlimited.



Sandia National Laboratories

Issued by Sandia National Laboratories, operated for the United States Department of Energy by Sandia Corporation.

NOTICE: This report was prepared as an account of work sponsored by an agency of the United States Government. Neither the United States Government, nor any agency thereof, nor any of their employees, nor any of their contractors, subcontractors, or their employees, make any warranty, express or implied, or assume any legal liability or responsibility for the accuracy, completeness, or usefulness of any information, apparatus, product, or process disclosed, or represent that its use would not infringe privately owned rights. Reference herein to any specific commercial product, process, or service by trade name, trademark, manufacturer, or otherwise, does not necessarily constitute or imply its endorsement, recommendation, or favoring by the United States Government, any agency thereof, or any of their contractors or subcontractors. The views and opinions expressed herein do not necessarily state or reflect those of the United States Government, any agency thereof, or any of their contractors.

Printed in the United States of America. This report has been reproduced directly from the best available copy.

Available to DOE and DOE contractors from
U.S. Department of Energy
Office of Scientific and Technical Information
P.O. Box 62
Oak Ridge, TN 37831

Telephone: (865) 576-8401
Facsimile: (865) 576-5728
E-Mail: reports@adonis.osti.gov
Online ordering: <http://www.osti.gov/bridge>

Available to the public from
U.S. Department of Commerce
National Technical Information Service
5285 Port Royal Rd.
Springfield, VA 22161

Telephone: (800) 553-6847
Facsimile: (703) 605-6900
E-Mail: orders@ntis.fedworld.gov
Online order: [http://www.ntis.gov/help/ordermethods.asp?loc=7-4-](http://www.ntis.gov/help/ordermethods.asp?loc=7-4-0#online)

[0#online](#)



SAND2005-2638
Unlimited Release
Printed September 2006

Final Report on Development of Pulse Arrested Spark Discharge (PASD) for Aging Aircraft Wiring Application

R. Kevin Howard, Steven F. Glover, Gary E. Pena, Matthew B. Higgins,
Larry X Schneider and Thomas R. Lockner

Applied Electromagnetic Technologies
Department 1643

Sandia National Laboratories
P.O. Box 5800
Albuquerque, NM 87185-1153

ABSTRACT

Pulsed Arrested Spark Discharge (PASD) is a Sandia National Laboratories Patented, non-destructive wiring system diagnostic that has been developed to detect defects in aging wiring systems in the commercial aircraft fleet. PASD was previously demonstrated on relatively controlled geometry wiring such as coaxial cables and shielded twisted-pair wiring through a contract with the U.S. navy and is discussed in a Sandia National Laboratories' report, SAND2001-3225 "Pulsed Arrested Spark Discharge (PASD) Diagnostic Technique for the Location of Defects in Aging Wiring Systems." This report describes an expansion of earlier work by applying the PASD technique to unshielded twisted-pair and discrete wire configurations commonly found in commercial aircraft. This wiring is characterized by higher impedances as well as relatively non-uniform impedance profiles that have been found to be challenging for existing aircraft wiring diagnostics. Under a three year contract let by the Federal Aviation Administration, Interagency Agreement DTFA-03-00X90019, this technology was further developed for application on aging commercial aircraft wiring systems. This report describes results of the FAA program with discussion of previous work conducted under U.S. Department of Defense funding.

Acknowledgements

The authors would like to acknowledge the Federal Aviation Administration's William J. Hughes Technology Center for supporting the development of PASD for applications in aircraft wiring systems. In particular, we thank Rob Pappas, Mike Walz and Cesar Gomez for their support of this work. The authors also acknowledge contributions by Parris Holmes Jr., Michael L. Horry and Michael A. Dinallo of the Applied Electromagnetics Department 1653 at Sandia National Laboratories, Albuquerque, New Mexico.

Table of Contents

I. Introduction	7
II. Background	8
III. Non-Destructive Nature of PASD	12
a. Overview	12
b. Measurements of Power and Impedance Profiles of PASD Discharges.....	12
c. Experiments.....	13
Breakdown voltage variation over multiple PASD pulses	13
Effect of PASD on low energy Voltage Breakdown	14
Effect of High Energy Discharge on low energy Voltage Breakdown.....	15
Microscopic Comparison of Insulator damage	16
IV. The Ability of PASD to Locate Aircraft Wiring Defects.....	20
a. Overview	20
b. PASD Applied to Aircraft Wiring with Defects	21
V. PASD Adaptations for Application to Aircraft Wiring Systems	29
a. Overview	29
b. Conversion to a Blumlein Style Pulser	29
c. Current Monitoring versus E-Dot Voltage Monitoring	30
d. Pulse Width Adjustment Modification	30
e. Pulse Width Optimization	32
f. Multi-Pulse Performance Investigation	34
VI. Commercialization of PASD	35
VII. Summary	36
VIII. References.....	37
IX. Distribution.....	38

Table of Figures

Figure 1: Illustration of PASD concept	8
Figure 2: PASD Charge line pulser	9
Figure 3: Abrasion on coaxial cable	9
Figure 4: Waveform illustrating PASD application on the wiring defect in figure 3.....	10
Figure 5: Input (blue), transmitted (black) and reflected (red) pulses.	13
Figure 6: Arc impedance history.....	13
Figure 7. Breakdown voltage and deposited energy versus shot number for 8 samples .	14
Figure 8: Example of low energy voltage breakdown distribution before application of PASD pulse.	15
Figure 9: Example of low energy voltage breakdown distribution after application of PASD pulse.....	15
Figure 10: Example of high energy voltage breakdown distribution before application of PASD pulse.	16
Figure 11: Example of high energy voltage breakdown distribution after application of PASD pulse.....	16
Figure 12: Microscopic photograph of a mylar sample before a low energy pulse.....	18
Figure 13: Microscopic photograph of a mylar sample after a low energy pulse.....	18
Figure 14: Microscopic photograph of mylar sample before PASD pulse.....	18
Figure 15: Microscopic photograph of mylar sample after PASD pulse.....	18
Figure 16: Microscopic photograph of mylar sample before high energy pulse.	18
Figure 17: Microscopic photograph of mylar sample after high energy pulse.	18
Figure 18: High voltage electrode following insulation material testing.	19
Figure 19: Wire to wire defect on unshielded twisted-pair aircraft wiring 63.3 feet down a 100 foot wire.....	22
Figure 20: Defect easily detected and located with PASD applied to defect of Figure 19.	22
Figure 21: Insulation defect in discrete wire.....	23
Figure 22: Insulation defect fixed to conductive ground plane.	23
Figure 23: PASD diagnostic waveform resulting from application to defect of figure 22.	23
Figure 24: Wire to wire defect.....	24
Figure 25: PASD diagnostic waveform for the defect of figure 24.....	24
Figure 26: Discrete wire with defect as seen in figure 22 located at 25ft. 8in.....	25
Figure 27: Discrete wire with defect as seen in figure 24 located at 25ft. 8 in.....	25
Figure 28: AANC Wiring Test Bed.....	26
Figure 29: PASD diagnostic waveform on Wiring Test Bed. 10 foot wire harness with defect at 8 ft.	27
Figure 30: PASD diagnostic on Wiring Test Bed. 10 foot wire harness with defect at 1.66ft.	27
Figure 31: Modeled data from 100 foot unshielded twisted-pair	33
Figure 32: Measured pulse data from 100 foot unshielded twisted-pair wiring.....	33
Figure 33: Detection of a wire to wire insulation chafe defect utilizing multi-pulsing technique.....	34

I. Introduction

Many available aircraft electrical wiring interconnect system (EWIS) diagnostic systems effectively detect and locate short and open conditions in aircraft wiring. These systems primarily rely on Time Domain Reflectometry (TDR), Standing Wave Reflectometry (SWR), or wiring Resistance and Capacitance (RC) measurements to detect and open or short condition. “Hi-Pot” test diagnostics have the ability to detect some insulation type defects, but they are unable to *locate* the detected defect. In general, EWIS diagnostics are ineffective or perform poorly when attempting to identify insulation related defects outside of open or shorted conditions.

The Department of Energy (DOE), the U.S. Navy, and the Federal Aviation Administration (FAA) have funded research and development at Sandia National Laboratories in a novel wiring system diagnostic called Pulsed Arrested Spark Discharge (PASD). The PASD concept and technique was first demonstrated on electrical wiring systems in 1996 under a DOE sponsored Nuclear Energy program. Sandia’s success during initial development of PASD for the DOE led to a contract with the U.S. Navy to explore the use of this concept for complex wiring in control and power systems. This work, completed in August 2001, demonstrated the ability of this technique to identify and locate gross defects and very difficult small-volume dielectric defects in a laboratory environment¹. This foundational work with PASD led to a three-year FAA program beginning in October 2002 with a focus on commercial aircraft wiring systems, a reduction to practice of the PASD technique, and near-term commercialization. This work was completed ahead of schedule. PASD has demonstrated great potential to locate aircraft wiring flaws relevant to aging processes, manufacturing defects, and installation damage.

This report will discuss the development status of PASD at the completion of the three year FAA program. Topics will include an operational overview of the PASD technology, non-destructive test results utilizing PASD, PASD’s effectiveness on aircraft wiring, PASD technology adaptation to facilitate application to aircraft wiring systems, and a discussion of the path towards commercialization of the PASD technology.

II. Background

Conventional TDR techniques launch a low voltage pulse down a transmission line and monitor the same injection point for reflected voltage pulse signals. Based on transmission line theory⁵, these signal reflections give an indication of the impedance characteristics down the length of the transmission line. PASD utilizes this same principle to get a “fingerprint” of the impedance characteristics of the transmission line with a relatively low voltage pulse of 100V. The voltage of the launched pulse is then incrementally increased from 1kV to 15kV while monitoring the waveform for changes. If an insulation defect of sufficient severity exists, the high voltage pulse will breakdown the air between the conductors creating a low-impedance short. A spark discharge, similar in energy to a common electrostatic discharge, will result in less than 100mJ² of deposited energy. Breakdown of the air results in an impedance discontinuity at the defect site, which in turn causes a reflection of the pulse. At the injection end of the transmission line, this impedance change, due to the air gap breakdown, will be seen as a change in the normalized waveform compared to the baseline pulse waveform. This change can therefore be measured in time using slightly modified TDR techniques to identify the defect location distance down the length of the transmission line.

Figure 1 is a block diagram of the PASD system. The pulser generates a high-voltage, low-energy (<100mJ²), short pulse that is injected into the wire under test. Sensors are located at the injection end of the wire. The defect in the insulation of the wire under test creates an airgap to an adjacent conducting return path (another wire or groundplane). The breakdown and the reflection off the breakdown site are seen in Figure 1.

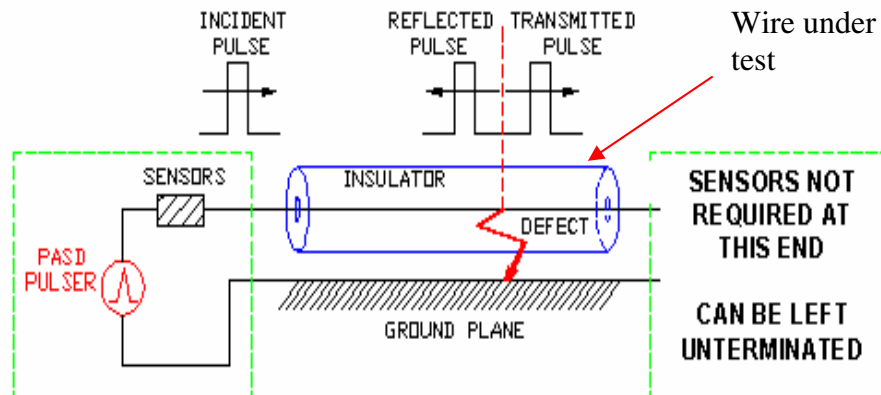


Figure 1: Illustration of PASD concept

Electric Field
(E-Dot) Sensor

Wire under
test

PASD
interface
cable

Charge line
pulser unit



Figure 2: PASD Charge line pulser

Figure 2 is a picture of a charge line pulser version of PASD. The pulser is contained in a sealed electrical box with insulating oil enabling the 25kV voltage holdoff. The electric field sensor (E-Dot) is pictured above and provides dE/dt data for analysis. Not pictured are the 30kV high voltage power supply and the digitizer (Tektronix TDS684 oscilloscope). This is strictly a laboratory pulse source. No attempt was made at this time to create a compact pulser.

Figure 3 and Figure 4 illustrate wiring damage investigated under the Navy program and the resulting waveforms.



Figure 3: Abrasion on coaxial cable

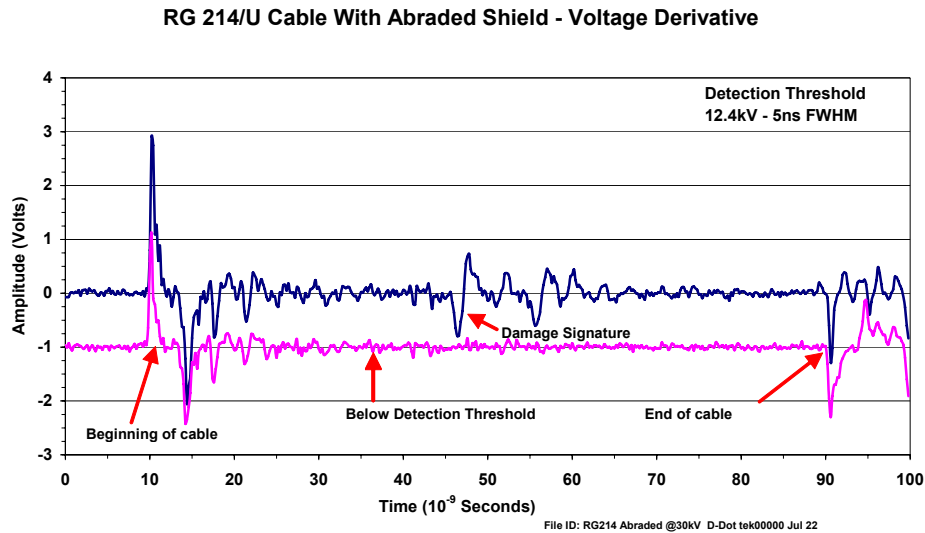


Figure 4: Waveform illustrating PASD application on the wiring defect in Figure 3.

In Figure 4 a typical raw PASD waveform is shown. The bottom pink waveform represents the low voltage baseline “fingerprint” of the cable under test. The top blue waveform results from a high voltage pulse that causes a break down in the air gap between the two conductors. This voltage waveform is sensed by a capacitively-coupled voltage probe, resulting in the derivative of the monitored voltage. The first deflection in the waveform represents the beginning of the cable and the last deflection to the right is a reflection from the end of the cable. The time difference between these two events represents the temporal length of the cable at 80ns. The abrupt impedance change at the defect site due to the arc breakdown can be easily seen. This change occurs approximately halfway down the length of the cable. The calculated location was 11.7 ft down a 25.8 ft. cable and the actual defect was located at 10.5 ft. Techniques to improve PASD’s location accuracy are described in later work. This example illustrates the PASD concept prior to the efforts under this FAA contract.

The goal of the FAA contract with Sandia National Laboratories was to refine the PASD concept into a system that could be used on aging commercial aircraft and develop a viable product commercialization partner. Many technical issues required investigation to insure PASD could be effective in this environment. First, PASD would have to be characterized on discrete wiring systems with relatively uncontrolled wiring geometries that result in severe impedance discontinuities down the length of the wire. This erratic impedance profile is quite different than the controlled impedances designed in coaxial and even shielded twisted-pair wire types that were previously investigated. These impedance fluctuations cause many signal reflections and attenuation which impede propagation of a pulse down a wire.

A modification to increase the output impedance of the PASD pulser was required to more closely match the characteristic impedance of the discrete aircraft wiring systems. By matching the impedances, reflections at the pulser and test cable junctions would be minimized and maximum power transfer could be achieved.

Determination of the maximum length of aircraft wiring that could be tested effectively with PASD technology was the next issue. Attenuation of the injected PASD pulse increases with increased wire length. This impacts the ability of the pulse to breakdown the air gap at defect sites limiting the effectiveness of the PASD technique on longer lengths of wiring.

The viability of the PASD concept depended on the premise that the injected energy was low precluding damage to the electrical properties of the wiring under test. The first objective completed under the three year FAA program was to insure PASD would not cause damage to wiring insulation.

III. Non-Destructive Nature of PASD

This section is provided as a summary of the detailed report “Assessment of the Non-Destructive Nature of PASD on Wire Insulation Integrity²”. For more detail on the experimental setup and data, the reader is referred to Sandia National Laboratories report SAND2003-3430.

a. Overview

PASD utilizes a propagating high voltage pulse to interrogate the insulation between two conductors. PASD must perform its test without causing damage to good insulation or further damage to anomalies within the wiring system. The first issue that required understanding was the behavior of the PASD pulse, the amount of energy deposited into the arc of a voltage breakdown due to the PASD pulse, and characterization of the impedance profile across an airgap during voltage breakdown due to the PASD pulse.

Three methods were used to assess PASD’s effect on wiring insulation. First, the breakdown history over multiple PASD pulses on the same surface was evaluated. If the PASD pulse deteriorates the insulation surface, reduced breakdown voltage strength would be expected on subsequent testing. The voltage breakdown process is statistical in nature; therefore, multiple samples were tested to collect adequate data. Second, it would be important to know the damage threshold in order to determine the safety margin of the technique. Experiments were performed to determine surface breakdown energy levels that cause damage to typical electrical insulation materials. Finally, microscopic comparisons of insulator samples exposed to the voltage breakdown conditions above were performed. Photographs of the insulator samples before and after the voltage breakdown exposure were compared.

b. Measurements of Power and Impedance Profiles of PASD Discharges

The first requirement for evaluating the non-destructive nature of PASD was to understand the energy deposited in the PASD discharge and the impedance profile of the airgap experiencing voltage breakdown. Figure 5 depicts the input, reflected and transmitted voltage pulses of a typical PASD discharge as well as the power deposited into the discharge arc. The energy deposited into the PASD discharge can be seen to be very low when the time width of the power pulse is considered.

Figure 6 shows a typical impedance profile for a PASD discharge. Until the applied voltage reaches a sufficient level to initiate electron avalanche breakdown, the impedance across the insulator gap is very high. The impedance of the gap collapses within 2-3 ns resulting in an arc discharge. This rapid impedance collapse is important to the functionality of the PASD concept and causes a distinct change in the impedance at the defect site. This sharp impedance discontinuity yields a distinct voltage reflection at this discharge point. This reflection is detected by the PASD sensors providing a distinct signal that can easily be interpreted to detect and locate defects.

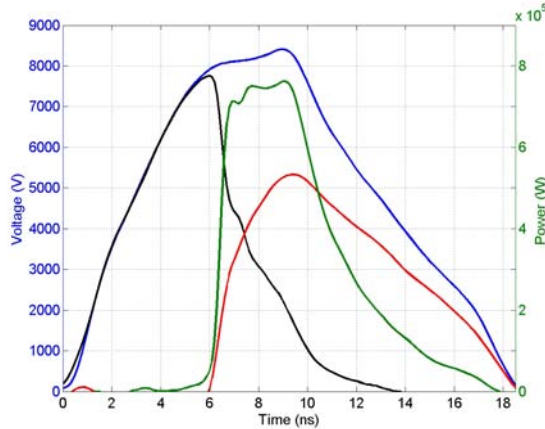


Figure 5: Input (blue), transmitted (black) and reflected (red) pulses. Also shown is the power pulse into the arc (green).

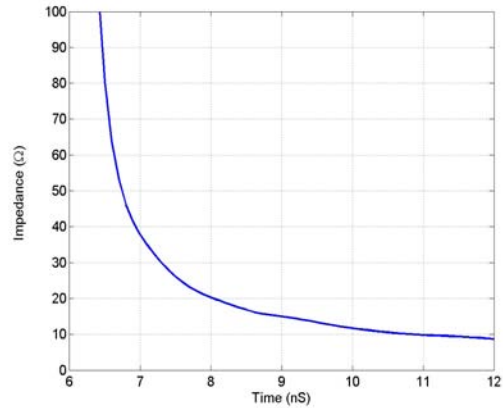


Figure 6: Arc impedance history.

c.Experiments

To characterize the non-destructive nature of PASD three experiments were performed. First the breakdown voltages of several common insulating materials over repeated PASD pulse applications were recorded and monitored for change. Second, an experiment to assess the PASD pulse’s effect on low energy voltage breakdown values of insulation was conducted. Finally, an experiment to assess the effect of a high energy pulse (much higher than that of PASD) on low energy voltage breakdown values of insulation was performed.

Breakdown voltage variation over multiple PASD pulses

Four different insulating materials (see Table 1) were exposed to the PASD pulse. For each material, 10 new samples were used and a series of 20 pulses were applied to each. Degradation of the insulation would be indicated by a drop in breakdown voltage after the first pulse application, or by a continuous degradation in the breakdown strength with successive pulse applications to the sample.

Table 1. Insulator materials and their thickness.

Material	Thickness
Celluloid	0.003-0.005 inches nominal
Mylar	0.003 inches
Teflon	0.03 inches
Polypropylene	0.06 inches

Results for 10 typical 20-shot runs are shown in Figure 7. In this figure, the breakdown voltage and energy deposited into the discharge are plotted versus shot number. The variation in breakdown voltage is statistical in nature. Note that there is no significant change in breakdown voltage after the first shot, and no trend towards lower voltage as the shot series progresses. This is a clear indication that no significant damage is occurring to the insulator surface under test from the PASD arc discharge².

As can be seen in Figure 7, the maximum energy absorbed was fairly consistent ranging from 3.45mJ to 6.31mJ for the celluloid with all other materials falling between these values. This is an energy level consistent with common static electricity shock a person might receive after walking across a nylon carpet.

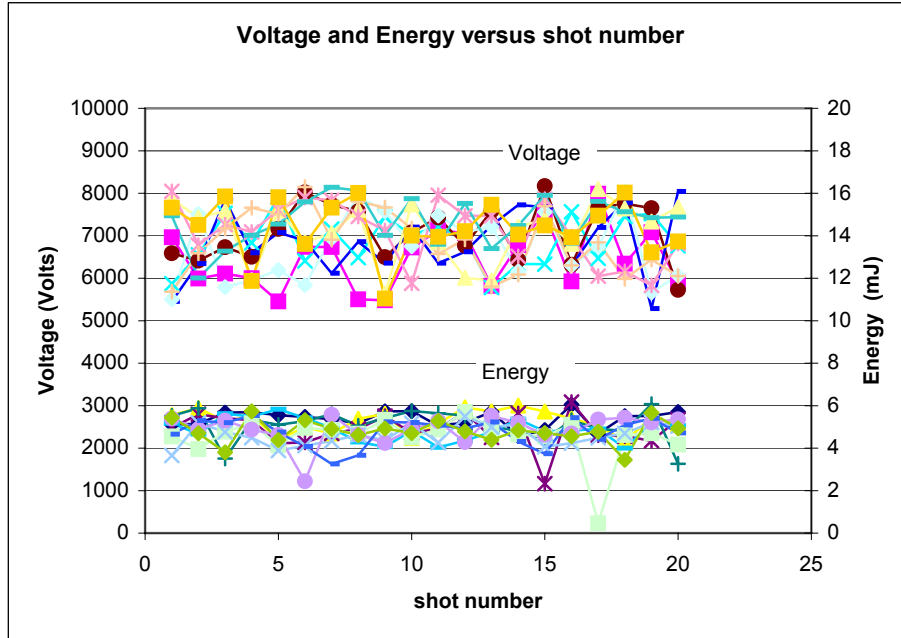


Figure 7. Breakdown voltage and deposited energy versus shot number for 8 samples

Effect of PASD on low energy Voltage Breakdown

The previous section investigated the effect of multiple PASD pulses upon the breakdown strength of the insulators. This section investigates the effect of a single PASD pulse upon the low energy breakdown voltage of an insulator. Low energy in this case was defined to be arc energy at least an order of magnitude less than that of the PASD pulse². The energy was limited by a high output resistance power supply setup that provided current limiting.

For these tests a single material was used, mylar with a 3 mil thickness. To investigate the effect of PASD pulse upon the voltage breakdown of the mylar samples, the following process was followed.

1. Insert a new insulator sample into the arc test fixture.
2. Initiate low energy breakdown using slowly rising DC voltage. Repeat 20 times to establish statistical average.
3. Conduct 1 PASD pulse experiment upon the sample using an 8kV pulse.
4. Initiate low energy breakdown using slowly rising voltage. Repeat 20 times to establish statistical average.

Sample results of this experiment can be seen in Figure 8 and Figure 9. Figure 8 shows very repeatable voltage breakdown data collected across the mylar sample surface due to a slowly increasing voltage. Twenty iterations of this procedure were performed to obtain a statistical average. The sample was then subjected to an 8kV PASD pulse. Figure 9 depicts the voltage breakdown data collected across the mylar sample surface due to a slowly increasing voltage after the PASD pulse. More variation can be seen in this data, but the increase in average voltage breakdown is the significant detail. This increase in voltage is a common phenomenon caused by conditioning of the anode and cathode electrodes as well as the insulator surface. The overall results of this testing yielded no consistent change in breakdown voltage values before and after application of the PASD pulse². This is an indication that PASD does not degrade the dielectric strength performance of an insulator.

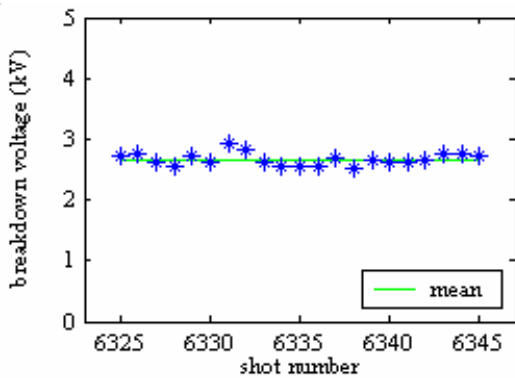


Figure 8: Example of low energy voltage breakdown distribution before application of PASD pulse.

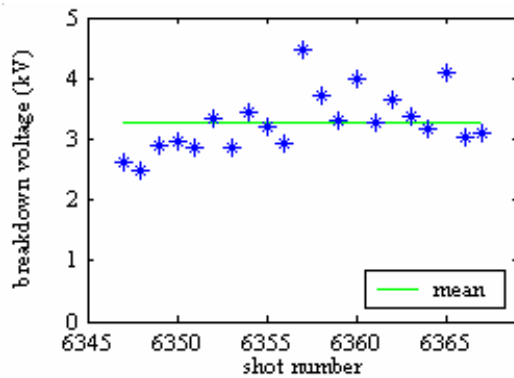


Figure 9: Example of low energy voltage breakdown distribution after application of PASD pulse.

Effect of High Energy Discharge on low energy Voltage Breakdown

The next step was to investigate the effect of high energy discharge, much higher than that of PASD, upon the dielectric strength of a mylar sample. This would provide an indication of the margin we have with the PASD pulse. This experiment utilized an experimental setup that provided a high energy pulse that exceeded that of PASD by at least an order of magnitude². The same procedure utilized in the low energy experiment above was implemented with the high energy version.

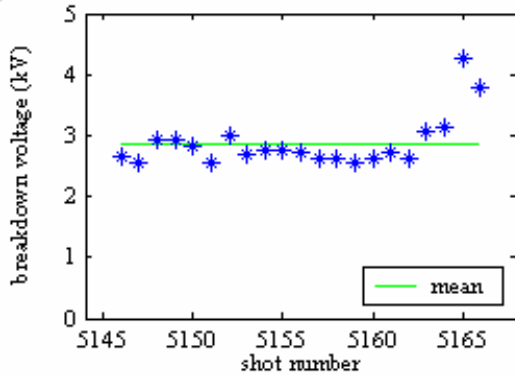


Figure 10: Example of high energy voltage breakdown distribution before application of PASD pulse.

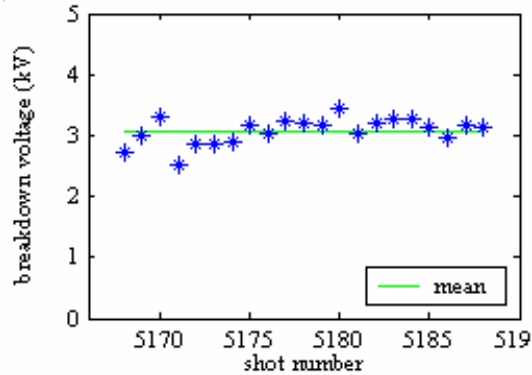


Figure 11: Example of high energy voltage breakdown distribution after application of PASD pulse

As can be seen in the typical results shown in Figure 10 and Figure 11, the data obtained from the high energy experiments suggest no pattern of change to the average breakdown voltage due to a high energy discharge. In two tests the average breakdown voltage stayed about the same, in one of the tests the average breakdown voltage increased, and in the remaining two tests the average breakdown voltage decreased. The lack of consistent significant reduction in the voltage breakdown of the insulator indicates that the high energy pulse, much higher than that of PASD, does not cause degradation to the insulation materials². This provides a good safety margin against insulation damage due to the PASD pulse.

Microscopic Comparison of Insulator damage

The previous sections on the effects of PASD pulses and high energy discharge on voltage breakdown yielded no trend of breakdown voltage reduction. This section documents the optical inspection of the insulation sample surfaces pre and post experiment.

Figure 12 through Figure 17 show photographs of mylar samples taken before and after discharge tests. The bending and deformation of the samples around the edges is a result of being placed in the test fixture and is independent of the voltage breakdown occurring across the samples. This deformation is more easily seen in some photographs than others and is dependent upon the lighting.

Figure 12 and Figure 13 contain photographs of a mylar sample before and after a low energy discharge. Notice the contamination (specs) apparent in Figure 13 following the low energy discharge. Since this contamination is located in areas not in the discharge path, they were likely in the fixture prior to the test. The important item to note is the lack of evidence in the photograph of insulator damage as a result of the discharge.

Figure 14 and Figure 15 contain photographs of a mylar sample before and after a PASD pulse. Notice the contamination (specs) apparent in Figure 15 following the PASD pulse. This contamination is significantly less than the contamination apparent in Figure 13. It is unclear whether the PASD pulse removed some of the contamination or if there was less contamination in the fixture during the test. Again the important item to note is the lack of evidence in the photograph of insulator damage as a result of the discharge.

Figure 16 and Figure 17 contain photographs of a mylar sample before and after a high energy discharge. Notice the material deposition apparent in Figure 17. This material deposition is suspected to be metal removed from the BNC connector pin evident in Figure 18. The deposition characteristics are not consistent with those of arc tracking due to insulation carbonization.



Figure 12: Microscopic photograph of a mylar sample before a low energy pulse.



Figure 13: Microscopic photograph of a mylar sample after a low energy pulse.

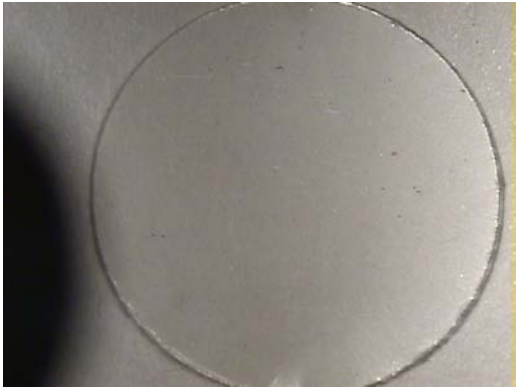


Figure 14: Microscopic photograph of mylar sample before PASD pulse.



Figure 15: Microscopic photograph of mylar sample after PASD pulse.



Figure 16: Microscopic photograph of mylar sample before high energy pulse.



Figure 17: Microscopic photograph of mylar sample after high energy pulse.



Figure 18: High voltage electrode following insulation material testing.

Based on the data obtained from this testing, it is believed that the PASD pulse does not damage the insulator under test². There was no evidence of breakdown strength changes following PASD pulse application other than the expected statistical variation, no evidence of an effect upon the low energy breakdown voltage after a PASD pulse or the higher energy pulses, and microscopic inspection did not indicate any material deposition characteristic of high energy destructive tracking.

IV. The Ability of PASD to Locate Aircraft Wiring Defects

a. Overview

The PASD technique had been demonstrated effective in detecting and locating defects in coaxial cabling and shielded twisted-pair wiring under prior development programs. The mission of the three year Federal Aviation Administration contract was to investigate the effectivity of the PASD technique in detecting and locating defects on wiring configurations commonly found in aging commercial aircraft.

The wiring systems of commercial aircraft include coaxial and shielded twisted-pair types investigated previously as well as unshielded twisted-pair and discrete wire configurations. There are many wiring insulator types as well as thinner wiring insulator jackets. The unshielded twisted-pair and discrete wiring geometries prevent many wiring diagnostic systems from effectively detecting and locating wiring defects in aircraft wiring due to the uncontrolled impedance profiles they possess.

Coaxial cabling is designed to maintain a very uniform impedance profile. Shielded twisted-pair has good impedance uniformity characteristics, although not a good as coaxial cabling. The shielding of both configurations provides electrical coupling isolation from nearby conducting surfaces and wiring as well as uniform environment geometries for the conductors. The twist provides uniform gap spacing geometries between the two conductors. These wiring configurations are relatively friendly to wiring diagnostic systems compared to the unshielded twisted-pair and discrete wire configurations described next.

Unshielded twisted-pair and discrete wiring systems exhibit erratic impedance discontinuities due to their susceptibility to electrical coupling with adjacent wiring, close conductive bulkheads and other environmental factors common in aircraft wiring systems. Electrical coupling occurs to these structures causing erratic changes in the impedance profile. Aircraft wiring is also strapped in bundles with other conductors of varying types and uncontrolled geometries causing further degradation in the impedance profile. This wiring configuration was not designed for high frequency electrical signal propagation and is therefore difficult for reflectometry-based wiring diagnostics to analyze.

The reflectometry-based wiring diagnostic systems work by propagating an electromagnetic pulse containing high frequency energy down a transmission line. Based on transmission line theory, when the pulse encounters an impedance discontinuity a reflection of the propagating pulse is directed back to the injection end of the line. TDRs monitor the injection end of the line and create an impedance profile of the line based on these reflections. Wiring insulation defects cause changes in the impedance profile of the wiring and theoretically produce reflections that could be detected by reflectometry-based diagnostics. Unfortunately, the erratic impedance profiles of even defectless wiring configurations impede the ability of the diagnostic to discern these defects. For the reflectometry-based systems to be effective on this type of wiring, a baseline profile of a defectless wire must be available for comparison. With the environmental factors involved, this requires the particular wire under test be used for the baseline measurement which invokes a question of practicality.

PASD is a system that works differently than most reflectometry-based systems. The PASD system uses a high voltage pulse to change the impedance characteristics of the wire under test at an insulation defect site. This change is caused by high voltage breakdown of the air gap between the conductor of the wire under test and a conducting return path where the insulation between them has been damaged. The voltage breakdown causes a collapse of the impedance at the defect location and therefore a reflection. A baseline impedance profile is obtained using a low voltage pulse which can be compared the normalized high voltage impedance profiles. A difference signifies a change which corresponds to an insulation defect enabling voltage breakdown. This differencing technique allows PASD to discern between impedance irregularities caused by environmental factors and impedance discontinuities caused by voltage breakdown at insulation damage sites. Slightly modified Time Domain Reflectometry techniques can be used to calculate the location of the defect as a distance from the injection end of the wire under test.

b. PASD Applied to Aircraft Wiring with Defects

PASD was tested on an unshielded twisted wire pair mounted in a cable assembly containing many different types of wires. This unshielded twisted wire pair contained a wire to wire insulation defect at 63 feet 4 inches (see Fig 16). The wire was tested with the PASD technique resulting in the waveform seen in Figure 20. This is the standard waveform obtained from PASD and represents multiple low voltage waveforms that do not cause the air gap voltage breakdown superimposed on a normalized high voltage waveform that did cause a breakdown in the air gap. The defect signature in Figure 20 is very distinct and corresponds to a two-way transit time of the pulse of 182ns. The two-way temporal length of the 100 foot cable is noted in Figure 20 as 276ns, corresponding to a 2.76ns/ft. two way propagation delay time. To calculate the distance to the defect, the propagation delay time along with a pulse width correction factor of 9ns are used (see pulse width correction factor in Section V).

$$D = \frac{(182 \text{ ns} - 9 \text{ ns})}{2.76 \text{ ns} / \text{ft}} = 62.7 \text{ ft}$$

The calculation above locates the defect 6 inches short of its actual location and well within the two foot location accuracy generally accepted by the aging aircraft community. It should be noted that the 2.76ns/ft. propagation delay value varies under different wiring configurations and should be measured for each application to insure optimal location accuracy performance.

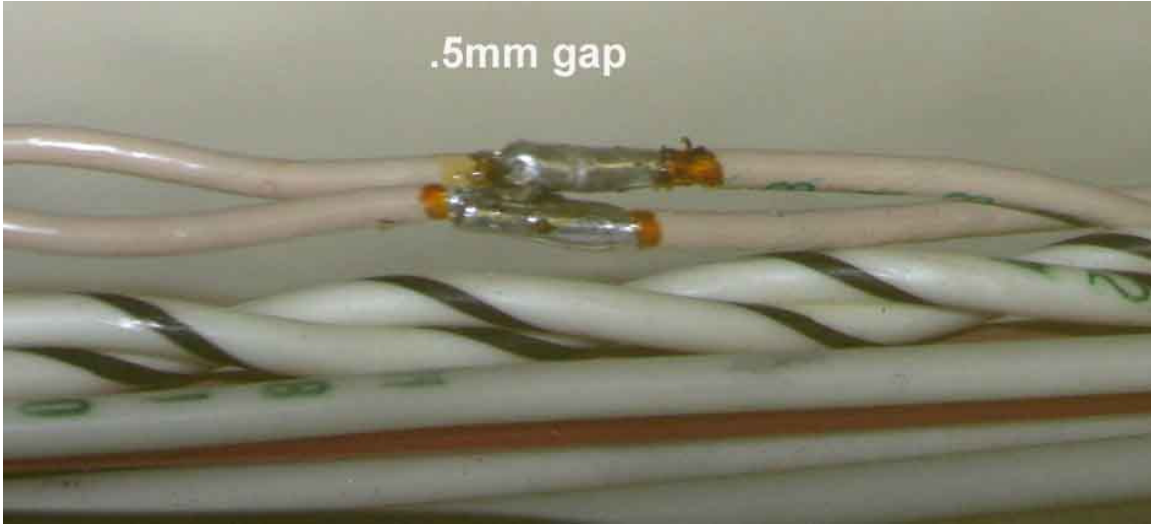


Figure 19: Wire to wire defect on unshielded twisted-pair aircraft wiring 63.3 feet down a 100 foot wire.

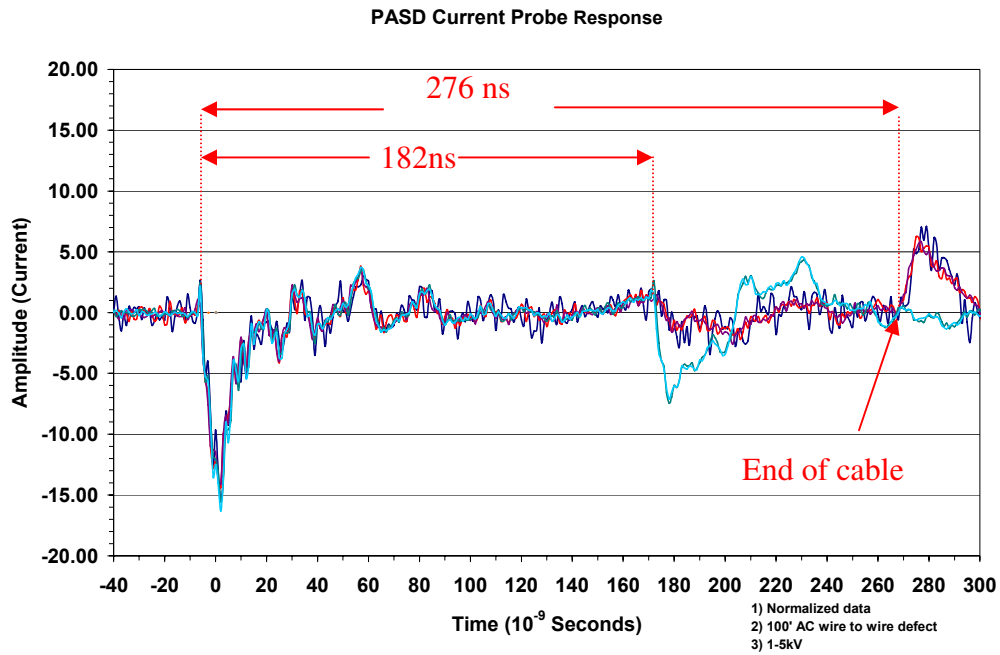


Figure 20: Defect easily detected and located with PASD applied to defect of Figure 19.

PASD was applied to a discrete wire configuration with a wire to ground type of defect. The defect (see Figure 21) was located 5 feet 8 inches down a 10 foot wire. It should be noted that this defect represents a very small volumetric defect that would not be detectable with standard reflectometry techniques. In Figure 23 the PASD diagnostic waveforms are seen. The defect is very clearly discernable as the superimposed low voltage baseline waveforms diverge from the normalized high voltage waveforms. This occurs at 26.8ns therefore:

$$D = \frac{(26.8ns - 9ns)}{3.1ns/ft} = 5.74ft$$

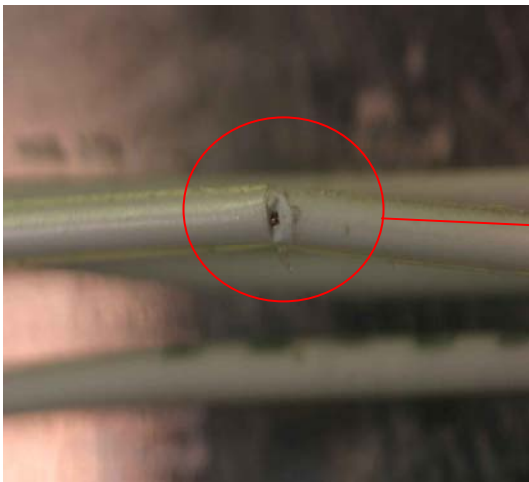


Figure 21: Insulation defect in discrete wire.

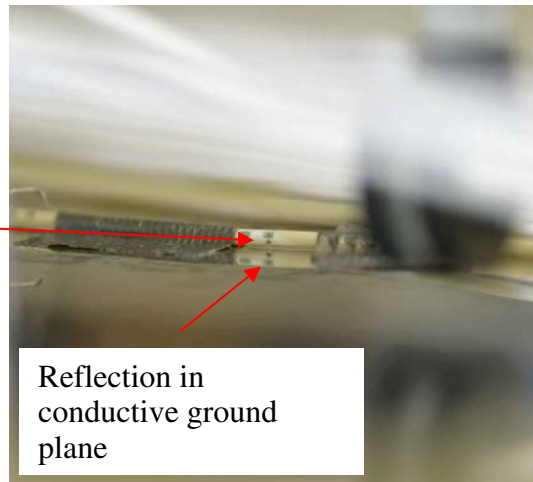


Figure 22: Insulation defect fixed to conductive ground plane.

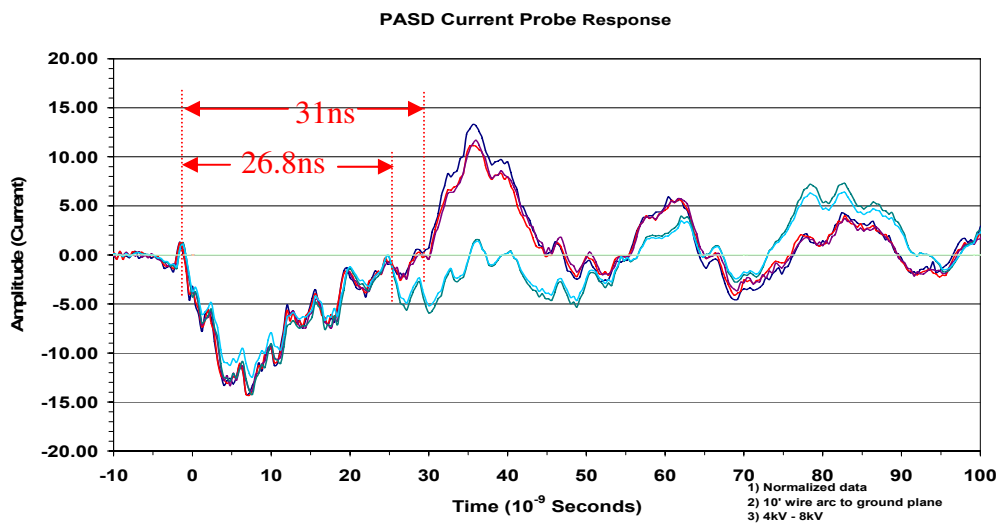


Figure 23: PASD diagnostic waveform resulting from application to defect of Figure 22.

The next aircraft wiring test documented in this report was a wire to wire type insulation defect as seen in Figure 24. This was a ten foot discrete wire configuration with the depicted defect located at 5 feet 8 inches. In Figure 25 the PASD diagnostic waveform depicts the cable with a temporal length of 31ns and a divergence of the baseline and breakdown waveforms at 23.6ns.

$$D = \frac{(23.6ns - 7.2ns)}{3.1ns / ft.} = 5.3ft.$$



Figure 24: Wire to wire defect

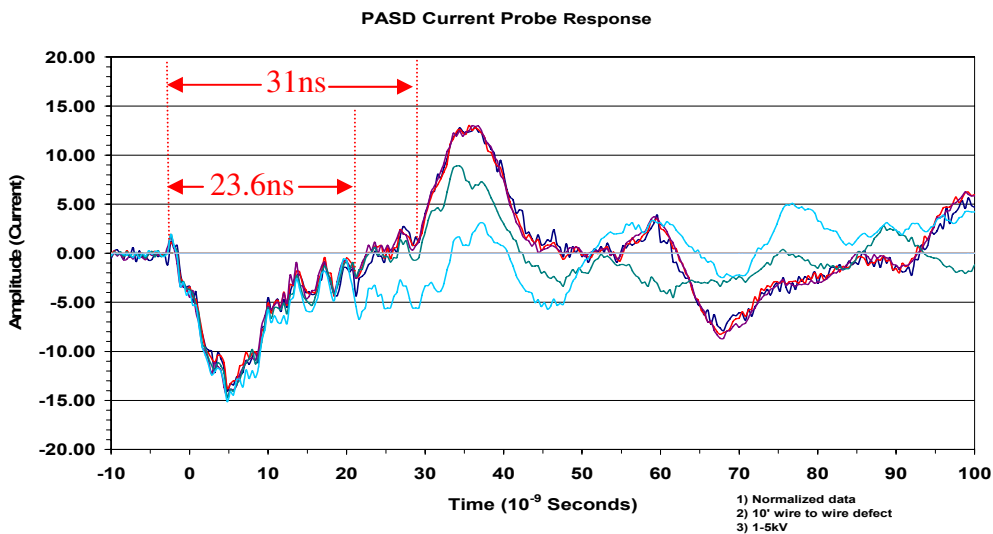


Figure 25: PASD diagnostic waveform for the defect of Figure 24.

The next two tests were similar defects as seen in Figure 22 and Figure 24 above on 50 foot wires. Both defects were located at 25 feet 8 inches. In Figure 26 the PASD diagnostic shows the 146.8ns temporal length of the wire. The baseline and voltage breakdown waveforms diverge at 84ns.

$$D = \frac{(84ns - 9ns)}{2.93ns / ft.} = 25.6 ft.$$

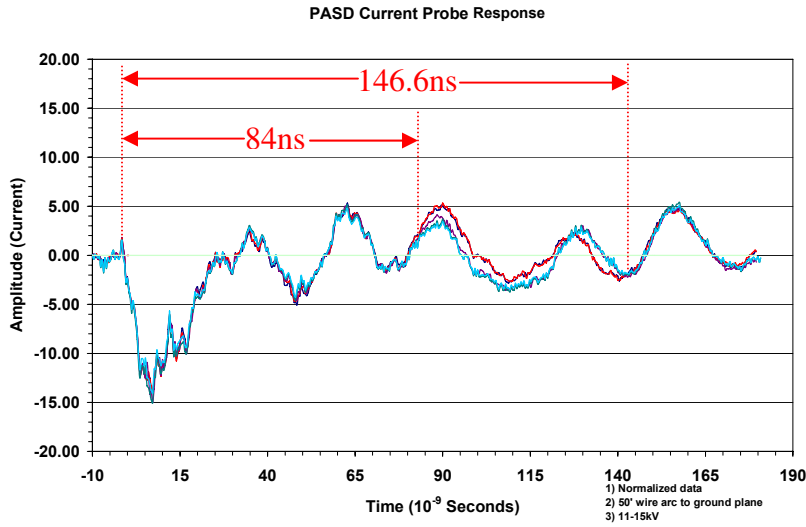


Figure 26: Discrete wire with defect as seen in Figure 22 located at 25ft. 8in.

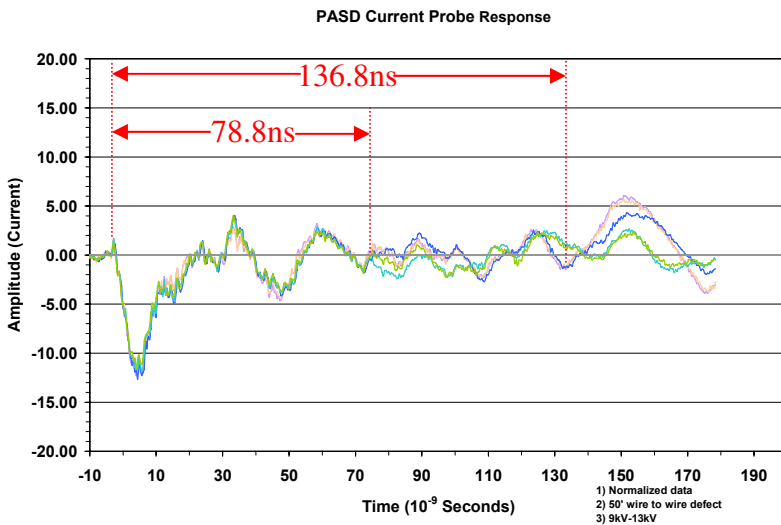


Figure 27: Discrete wire with defect as seen in Figure 24 located at 25ft. 8 in.

Figure 27 above depicts the PASD diagnostic waveforms from a defect like the in Figure 24 located 25 feet 8 inches down a 50 foot discrete wire configuration. The temporal two-way length of the wire is 136.8ns and a defect is noted at 78.8ns.

$$D = \frac{(78.8ns - 9ns)}{2.74ns / ft.} = 25.5 ft.$$

PASD was applied to a standard that other aircraft wiring system diagnostic manufacturers had been tested on, the AANC (Airworthiness Assurance Non-destructive testing Center) Wiring Test Bed³ (see Figure 28). This test bed contains over 80 harnesses, most of which were extracted from retired commercial aircraft, with various assortments of wiring defects fabricated into them. PASD is a wiring diagnostic designed to detect insulation type defects, therefore these defect types were the focus of the PASD system testing on the wiring test bed.



Figure 28: AANC Wiring Test Bed

The first AANC Wiring Test Bed defect diagnostic result presented was an insulation chafe defect located 1mm above the ground plane. Figure 29 shows the baseline waveform (blue) and the breakdown waveform (red) diverging at 84.4ns. This particular configuration included a 16 foot interface cable (44ns two way temporal length).

$$D = \frac{(84.4ns - 16ns - 44ns)}{3.1ns / ft.} = 7.9 ft.$$

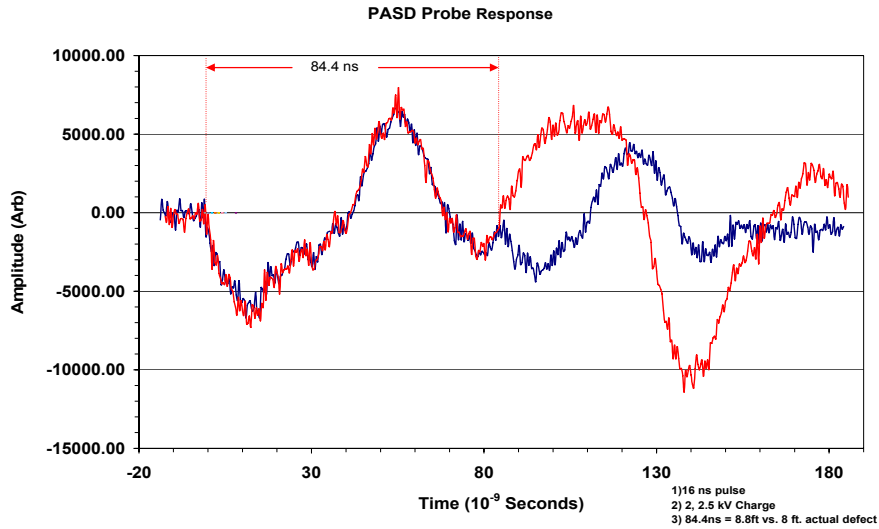


Figure 29: PASD diagnostic waveform on Wiring Test Bed. 10 foot wire harness with defect at 8 ft.

The second defect PASD diagnostic result from the AANC Wiring Test Bed was an insulation breach defect that was located 1mm above the ground plane. The defect was located 1 foot 8 inches into the 10 foot harness. Figure 30 depicts the PASD results with the baseline and breakdown waveforms diverging at 66ns.

$$D = \frac{(66ns - 16ns - 44ns)}{3.1ns / ft.} = 1.9 ft.$$

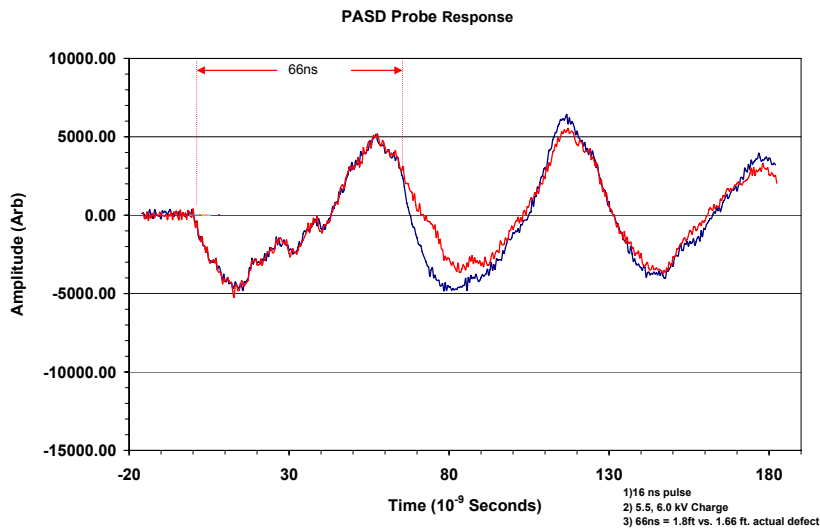


Figure 30: PASD diagnostic on Wiring Test Bed. 10 foot wire harness with defect at 1.66ft.

Many other insulation type defects were tested on the AANC Wiring Test Bed. Table 2 lists the three defect types tested as well as the gap between the conductor at the defect and the conducting return path. The insulation crack defect results are particularly difficult to detect with current wiring diagnostic technologies, but PASD was able to detect and locate 3 out of the 6 crack defects that were tested.

Table 2: PASD Results on AANC Wiring Test Bed

DEFECT	QTY	DEFECTS DETECTED	DEFECTS UNDETECTED
Insulation Chafe			
1mm gap	7	7	0
3mm gap	5	3	2
Insulation Breach			
1mm gap	2	2	0
3mm gap	6	3	3
Insulation Cracks			
1mm gap	6	3	3
3mm gap	1	0	1
TOTAL	29	17	12

In summary, the PASD diagnostic technique was successful detecting and locating insulation defects in commercial aircraft specification wiring. The aircraft wiring systems have an erratic impedance profile that makes detection of small volumetric insulation defects impossible by standard reflectometry techniques. Hi pot type testing can detect some of these defects, but is unable to locate the defect. The PASD technology, now adapted to aircraft wiring systems, was demonstrated capable of detecting as well as locating insulation defects in these systems.

In subsequent sections of this report the modifications that were made to PASD in order to facilitate application to aircraft wiring configurations are discussed. PASD will undoubtedly experience further changes and refinement as it is developed into a commercial product, but the science and major modifications were defined under this program.

V. PASD Adaptations for Application to Aircraft Wiring Systems

a. Overview

Under the FAA funded program the PASD technology was modified and improved for use on aircraft wiring systems that include more challenging wiring configurations with uncontrolled impedance profiles. The erratic impedance profiles found in aircraft wiring systems prohibit reflectometry technologies from being able to discern between actual defects and the normal impedance discontinuities caused by aircraft wiring environments and wiring geometries. PASD, with its reflectometry differencing technique, is immune to these discontinuous impedance profiles.

Several modifications were required in order to adapt the PASD system to commercial aircraft wiring systems. The output impedance of the PASD pulser needed to be increased to more closely match the characteristic transmission line impedance of discrete and unshielded twisted-pair wiring systems to allow maximum power transmission. The sensor monitoring the PASD pulse on the injection end of the diagnostic system required modification to facilitate monitoring of discrete wiring. The optimal pulse width required definition in order to maximize propagated voltage amplitude down the discrete wiring. These and other developments are discussed in this section of the report.

b. Conversion to a Blumlein Style Pulser

The heart of the PASD diagnostic system is the high voltage pulser that generates and injects the high voltage propagating pulse onto the wiring under test. The pulser of the previous work under DOE and U.S. Navy funding was a charge-line type pulser. This pulser system is capable of providing very fast rise-time square pulses. The drawback to the charge-line pulser system is maximum output pulse voltage amplitude that is half of the charge voltage applied. This forces a requirement of 30kV to obtain the 15kV maximum voltage amplitude pulse of PASD. The PASD pulser system prior to this FAA program featured a 50 ohm output impedance which further limited the output voltage amplitude when coupled into the approximately 120 ohm characteristic impedance of the discrete and unshielded twisted-pair wiring configurations of aircraft wiring systems.

The blumlein pulser was chosen to replace the charge-line pulser in the PASD system for the aircraft wiring version. This configuration of pulser features an output voltage pulse amplitude equal to the charge voltage applied. Furthermore, the output impedance of the blumlein pulser, with standard 50 ohm coaxial cabling, is doubled to 100 ohms which more closely matches the approximately 120 ohm characteristic impedance of the discrete and unshielded twisted-pair wiring.

The blumlein pulser configuration was fabricated and installed into the PASD pulser unit and yielded the higher voltage amplitude pulses that were expected.

c. Current Monitoring versus E-Dot Voltage Monitoring

The PASD system developed under previous work utilized an E-Dot sensor to monitor the propagating voltage pulses on the wire under test. This monitor facilitates capacitive coupling of the electric field of the propagating pulse onto a transmission cable. This type of sensor picks up rates of change in the electric field which can then be integrated and calibrated to present a real time voltage amplitude pulse waveform. This type of sensor is ideal for coaxial geometries, but not for the discrete wiring configurations found in aircraft electrical systems. Therefore a new sensor was required.

The Pearson Model 2877 Current Voltage Transformer was selected as the replacement sensor to replace the E-Dot sensors on PASD. With a usable rise time of 2ns and 100A peak current rating, this unit met the bandwidth and amplitude requirements.

This CVT is easily installed around the discrete wiring leads that feed into the wire under test in the PASD system. The output of the CVT is a real time current waveform. The current pulses sensed by the CVT are directly related to the voltage of the propagating pulses.

d. Pulse Width Adjustment Modification

PASD is able to locate wiring insulation defects by Time Domain Reflectometry techniques. Under the U.S. Navy program, PASD was able to locate some defects very accurately, but other defect location data was off by 10% or more (see Table 3). Investigation of this error yielded a pulse width adjustment procedure that corrected the data error to less than 3% (see Table 4).

The theory behind this correction is based in voltage breakdown of air gaps. The probability an air gap will ionize and allow current flow, as evidenced by an arc, is great when a certain voltage threshold is reached. For pulses less than one microsecond duration, when the product of the voltage and pulse width ($Vt^{1/6}$) exceed this threshold, voltage breakdown will occur^{3(p. 57)}. Rephrasing this concept intuitively, for short pulses, when a sufficient voltage is applied across an air gap for a sufficient amount of time, a breakdown will occur. The time factor in the PASD technique is fixed by the pulse width of the propagating pulse. The procedure for the PASD technique is first to obtain a baseline waveform at a voltage amplitude lower than the value needed for air gap breakdown. Then the voltage is raised slowly, while incrementally pulsing the wire under test, until the normalized waveform comparison to the baseline waveform indicates a change. This change is due to an air gap breakdown and indicates an insulation defect. It also indicates that the $Vt^{1/6}$ product has just exceeded the threshold at that defect site. This means that the entire pulse width of time is needed for the applied pulse amplitude to break down the air gap. Since the time for voltage breakdown of the air gap is at or very near the pulse width of the high voltage pulse, it is easy to see that with the PASD procedure a pulse reflected from a defect site would be delayed by approximately that pulse width time. In the case of voltage breakdown of the air gap between the conductor and the conducting return path, an adjustment of one pulse width is required. This adjustment can be seen in the data of section IV and was nominally 9ns or 16ns depending on the pulse width that was used in each test scenario.

Table 3: Location accuracy of PASD under U.S. Navy program

Cable Type and Damage	Cable Length (ft)	Damage/Defect Location (ft)	Signal Transit Time Location (ft)¹	Percent Agreement
RG-174 Break in shield	24	19.2	19.8	3.1
RG-214 Break in shield	30	22.9	23.4	2.2
Alpha 2473 (TP ²) insulation damage	30.3	24.2	25.6	5.8
Alpha 1772 (FC ³) insulation damage	30.3	20	22.3	11.5
RG-214 abraded shield & insulation	25.8	10.5	11.7	11.4
RG-174 abraded shield & insulation	24.3	13.8	14.5	5.1
RG-214 pin-in-Shield (1.2 mm)	30.3	8.4	9.3	10.7
RG-214 pin hole only (1 mm)	30.3	22.2	23.8	7.2
Nonuniform impedance (TP)	15.6	12	11.7 ⁴	2.5

1. Used Polyethylene Dielectric of (ϵ_r) 2.25.

2. TP – Twisted-pair.

3. FC – Four Conductor.

4. Used Effective Dielectric of (ϵ_r) 2.53.

Table 4: Pulse width correction applied to U.S. Navy data.

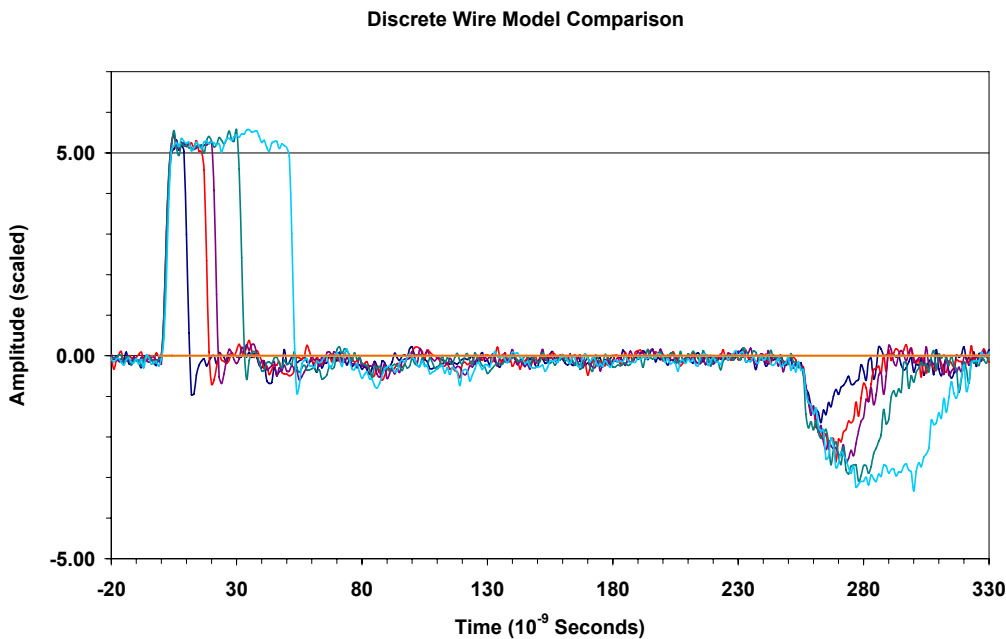
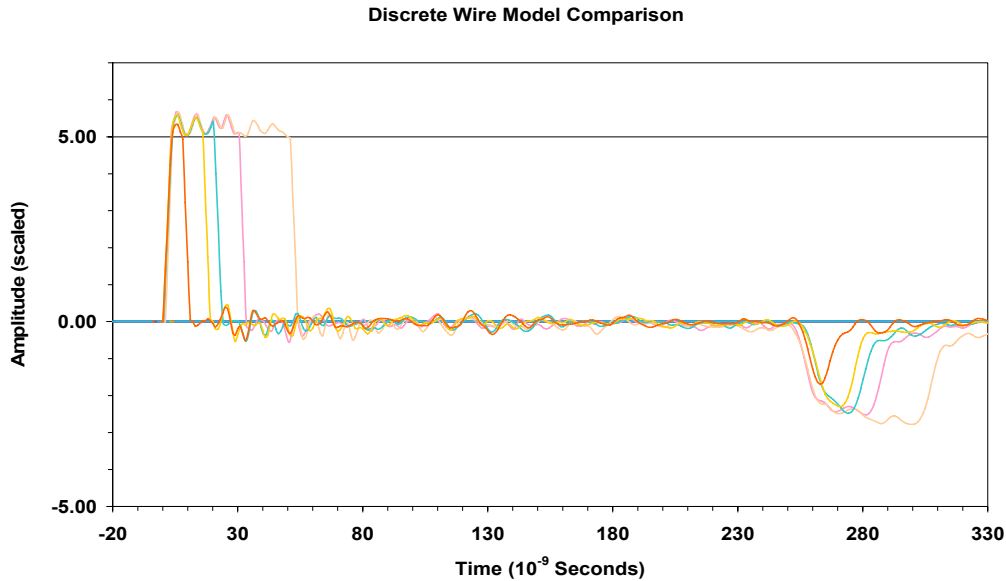
Cable Type and Damage	Cable Length (ft)	Damage/Defect Location (Actual) (ft)	PASD Transit Time Location (Adjusted) (ft)	Location Agreement (Adjusted) (%)	Location Agreement Originally Reported in SAND2001-3225² (%)
RG-174 Break in shield	24	19.2	19.2	Match	+3.1
RG-214 Break in shield	30	22.9	22.8	Match	+2.2
Alpha 2473 (TP) insulation damage	30.3	24.2	24.6	1.8	+5.8
RG-214 abraded shield & insulation	25.8	10.5	10.8	2.4	+11.4
RG-174 abraded shield & insulation	24.3	13.8	13.4	2.7	+5.1
RG-214 pin-in-Shield (1.2 mm)	30.3	8.4	8.5	Match	+10.7
RG-214 pin hole only (1 mm)	30.3	22.2	22.2	Match	+7.2
Non-uniform impedance (TP)	15.6	12	12.3	2.6	-2.5

e. Pulse Width Optimization

The pulse characteristics of the previous PASD pulser were adequate for the high frequency coaxial cabling and the relatively controlled impedance profiles of the shielded twisted-pair wiring. However, the discrete wire and unshielded twisted-pair wiring common in commercial aircraft wiring systems were not designed for high frequency propagation. The 5ns pulse width of the previous pulser system contains significant energy concentrations in the high frequency components of the pulse. A wider pulse provides higher concentrations of the energy in lower frequencies. The limiting factor is the desire to limit the amount of energy available to be deposited into the arc, thereby dictating shorter pulse widths.

A PSpice© model was developed to aid in optimization of the pulse width from the PASD pulser system. The input parameters to this model included conductor characteristics such as size and material parameters and insulation material properties. Another input parameter included was the gap spacing between the conductor and a nearby conducting return path. This provided the ability to model discrete and unshielded twisted-pair wiring responses to various pulse parameters. Figure 31 and Figure 32 show a comparison between the modeled unshielded twisted-pair wiring and actual data obtained from this configuration of wiring. The model predicted 30ns to be the optimum pulse width for 100 foot wiring applications. The measured data

obtained from pulsing a 100 foot unshielded twisted-pair wire in Figure 32 supported the 30ns pulse width selection. Later high voltage measurements with the PASD Pulser also confirmed the 30ns pulse width optimization for the 100 foot wiring configuration. Shorter wiring runs can be tested with shorter pulses, for instance a 30 foot wire can be adequately tested with the 16ns pulse width.



f. Multi-Pulse Performance Investigation

In early discussions of PASD technology and documented in the patent application, multi-pulsing was a technique of interest. If two pulses could be timed to arrive at a particular location simultaneously, the voltage at that point would be doubled and the probability for air gap breakdown and therefore defect detection would be increased. Another way of implementing multi-pulsing utilizes an initial, much longer pulse followed by the short PASD pulse. The theory behind this technique is that the longer pulse would “pre-polarize” the air gap between the two conductors promoting voltage breakdown by the PASD pulse at lower amplitude.

Under the FAA contract multi-pulsing was investigated. An insulation chafe between two conductors was fabricated 80 feet down a 100 foot cable. A 1mm gap was fixed between the two damaged wires. A long “pre-polarization” 2kV pulse was launched followed by a PASD pulse. The PASD pulse alone was unable to break down the gap (prior to optimization of the pulse width). With the multi-pulsing technique, the gap easily broke down at 8kV (see Figure 33). This was clear indication of the benefit of multi-pulsing with the PASD technology. More research into this technique is warranted in the future.

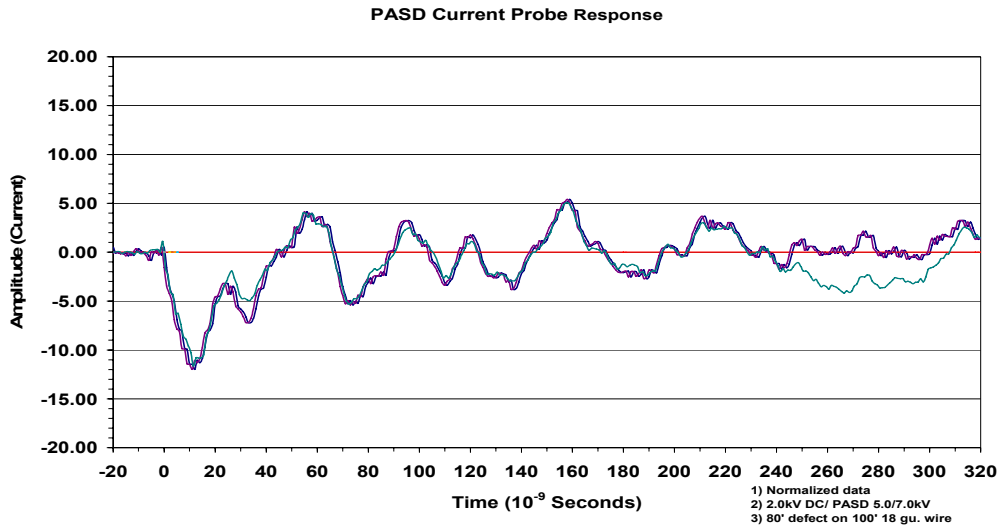


Figure 33: Detection of a wire to wire insulation chafe defect utilizing multi-pulsing technique.

VI. Commercialization of PASD

The PASD technique was discussed with several commercial entities capable of maturing a technology concept and demonstration unit into a viable commercial product with the type of features required by specific end users. This process of soliciting commercial partners, in general, proceeded very favorably. One of the most difficult aspects in this stage of technology transfer and commercialization is determining the commercial value of a given technology and the complete costs involved in final engineering and manufacturing. This process led to partnering with a corporation with significant experience in aviation industry electronics, knowledge of the market value of wiring diagnostic for aircraft systems, and the motivation and means to complete the transformation the PASD concept to a technically viable, profitable, commercial product. The final stage in the transition of PASD from an R&D concept to a product widely used in the aviation industry is licensing. Sandia Corporation was awarded a US Patent for PASD on Feb. 8, 2005, entitled "Method and Apparatus for Electrical Cable Testing By Pulsed Arrested Spark Discharge". The authors of the Patent first filed a Sandia Laboratories DISCLOSURE OF TECHNICAL ADVANCE on Oct. 30, 2001. The referenced company has acquired a Test and Evaluation license and has significantly matured the PASD technique towards a commercial product. Interest in this new diagnostic is growing rapidly as it stands alone in its capability to locate the type of defects seen in aircraft wiring systems. The final step towards commercialization now resides in the hands of this industrial partner, or other partners, willing to license the PASD concept from Sandia National Laboratories and to complete the final development of this diagnostic. Anticipated final engineering costs and manufacturing costs are expected to be very reasonable. PASD clearly has potential to be a significant new diagnostic for the commercial aircraft community as well as other aircraft or wiring systems where reliability needs to be verified.

VII. Summary

PASD is effective at detecting and locating a variety of insulation defects in complex wiring geometries. It is highly immune to line impedance variations, an important property in aircraft wiring systems, and has been shown to be nondestructive to electrical insulation materials. Due to the simplicity of the PASD concept, the low energy PASD pulser and diagnostics can be readily implemented into a portable diagnostic system. PASD shows great promise as an effective diagnostic to find difficult to locate insulation defects such as breached insulation, chaffing, and physically small insulation cracks. Although the PASD technique will likely evolve as it enters into field applications (pulse shape, testing strategy, etc.) it is capable of making a near-term impact on the ability of inspection and maintenance organizations to detect and locate potentially hazardous insulation defects

VIII. References

- [1] Dinallo, Michael A., Schneider, L. X, “Pulsed Arrested Spark Discharge (PASD) Diagnostic Technique for the Location of Defects in Aging Wiring Systems”, SAND2001-3225.
- [2] Glover, Steven F., Higgins, M.B., Pena, G.E., Schneider, L.X, “Assessment of the Non-Destructive Nature of PASD on Wire Insulation Integrity,” SAND2003-3430.
- [3] AANC Wiring Test Bed, <http://www.sandia.gov/aanc/WiringLabHome.htm>.
- [4] Pai, S.T., Zhang, Qi, “Introduction to High Power Pulse Technology”, World Scientific Publishing Co., 1995.
- [5] Paul, Clayton R., “Introduction to Electromagnetic Compatibility,” John Wiley and Sons, Inc., 1992.
- [6] Schneider, Larry X, Dinallo, M.A., Howard, R.K., Glover, S.F., Pena, G.E., Lockner, T.R., “Pulse Arrested Spark Discharge (PASD) Wiring Diagnostic,” presentation at the 8th Joint NASA/FAA/DOD Conference on Aging Aircraft, January 2005.
- [7] Howard, R. Kevin, Schneider, L. X, Dinallo, M.A., Pena, G.E., “Assessment of the Ability of PASD to Located Defects in Typical Commercial Aircraft Wiring”, SAND2005-2290.

IX. Distribution

2	MS9018	Central Technical Files, 8944
2	MS0899	Technical Library, 4536
1		Robert Pappas, AAR-480 Federal Aviation Administration William J. Hughes Technical Center Atlantic City International Airport Atlantic City, NJ 08405
1		Cesar Gomez, AAR-433 Federal Aviation Administration William J. Hughes Technical Center Atlantic City International Airport Atlantic City, NJ 08405
1		Michael Walz, AAR-433 Federal Aviation Administration William J. Hughes Technical Center Atlantic City International Airport Atlantic City, NJ 08405
4	MS1152	Larry Schneider, 1643
2	MS1152	Steven Glover, 1643
1	MS1152	Gary Pena, 1643
1	MS1152	Kevin Howard, 1643
1	MS1152	Mike Dinallo, 1643
1	MS1182	Tom Lockner, 15335
1	MS1152	Matt Higgins, 1643
1	MS1152	Kim Reed, 1643
1	MS1152	Roy Jorgenson
1	MS1152	Larry Warne